ASCERTAINING THE INFLUENCE OF GRID VS. NON-GRID TECHNIQUES ON RADIATION DOSE TO THE SKULL, EYES, AND THYROIDS AND IMAGE QUALITY IN ANTEROPOSTERIOR (AP) SKULL X-RAY EXAMINATIONS: A PHANTOM STUDY

INAYATULLAH SHAH SAYED, PhD (CORRESPONDING AUTHOR)
DEPARTMENT OF DIAGNOSTIC IMAGING AND RADIOTHERAPY, KULLIYYAH OF ALLIED HEALTH SCIENCES, INTERNATIONAL ISLAMIC UNIVERSITY MALAYSIA, JALAN SULTAN AHMAD SHAH, 25200 KUANTAN, PAHANG, MALAYSIA
inayatullah@iium.edu.my

FATIN AMIRAH BINTI ABDULLAH, BSc
DEPARTMENT OF DIAGNOSTIC IMAGING AND RADIOTHERAPY, KULLIYYAH OF ALLIED HEALTH SCIENCES, INTERNATIONAL ISLAMIC UNIVERSITY MALAYSIA, JALAN SULTAN AHMAD SHAH, 25200 KUANTAN, PAHANG, MALAYSIA
nadzatulakhma37@gmail.com

ABSTRACT

Introduction: Skull radiography plays a pivotal role in diagnosing traumatic head injuries, yet concerns persist regarding radiation exposure to organs, such as the brain, eyes, and thyroids. This study addresses the often-overlooked radiation protection measures for these organs, particularly in antero-posterior (AP) skull radiography cases. The utilization of a grid is essential for visualizing intricate cranial details, encompassing both soft tissues and bony structures. However, grid usage typically necessitates higher exposure settings compared to the non-grid technique. Thus, we investigate the effects of grid and non-grid techniques on entrance surface dose (ESD) to the brain, and radiation dose to the eyes and thyroid, and image quality. **Methods:** The Kyoto Kagaku Anthropomorphic PBU-50 head phantom was exposed with the Siemens Multix Top X-ray system. Various exposure parameters were explored, including (68 kVp, 9 mAs), (68 kVp, 12.5 mAs), (75 kVp, 9 mAs), and (75 kVp, 12.5 mAs). ESD for skull, eyes, and thyroid were measured using optically stimulated luminescence dosimeters (OSLDs) positioned at the glabella, eyes, and thyroid on the phantom. Image quality was assessed using the Image Criteria Score (ICS). **Results:** The analysis revealed that there was no significant difference in ESD between the grid and non-grid techniques when considering the larger OID ($p > 0.05$). However, a significant distinction in image quality emerged between the two techniques, especially for lower exposure factor ($p < 0.05$). Remarkably, the non-grid technique with a 4 cm air gap (OID) exhibited slightly higher ESD values in comparison to the grid technique (no air gap) when employing identical exposure parameters. **Conclusion:** Using the grid technique with no air-gap led to lower ESD values and better image quality, even at the lowest exposure settings. Additionally, this study found that the radiation dose values for the eyes and thyroid remained remarkably low for images attaining the highest ICS scores. These findings underscore the importance of optimizing radiographic techniques to achieve a balance between image quality and radiation dose for brain, eyes and thyroids in AP skull radiography.

Keywords: ESD, OSLD, OID, Grid, Skull examination, Exposure factors

INTRODUCTION

Medical imaging, including skull X-ray examinations, plays a crucial role in diagnosing diseases, localising abnormalities, and characterising pathologies (Karami et al., 2017). However, it is imperative to assess and justify the radiation dose and physical parameters applied to patients to ensure radiation protection in diagnostic radiology. Skull X-ray examinations, linked to low levels of radiation exposure, are now standard practice for patients who have had head injuries (IAEA, 2002). Skull x-ray radiography uses minimal doses of radiation, but repeated examinations on the same patient can nevertheless cause radiation overload. This could potentially contribute to the development of cancer and, in some cases, lead to cognitive issues in adulthood (Mazonakis et al., 2004). Often, healthcare practitioners may underestimate the radiation dose absorbed by these radiosensitive organs during skull x-ray examinations. Additionally, the omission or inadequate use of shielding can result in unnecessary radiation exposure to tissues. To address these concerns, European Diagnostic Reference Levels (DRLs) set maximum values for Entrance Surface Dose (ESD) for skull X-rays, emphasising the importance of dose optimisation (Mazonakis et al., 2004). Dose optimisation aims to use the minimum necessary radiation exposure without compromising image quality (Gogos et al., 2013), aligning with the As Low As Reasonably Achievable (ALARA) principle (Donya et al., 2014).

One aspect often overlooked during skull X-ray examinations is the radiation dose to the eyes and thyroid tissues. These tissues are particularly sensitive to radiation due to their actively dividing and less-differentiated cells. Proper patient preparation, including the use of lead shielding, can help achieve dose optimization. Unfortunately, many routine examinations do not provide patients with wearable safety shielding devices like thyroid shielding or eye covers (Fetterly et al., 2017).

Dose monitoring is essential to ensure radiation exposure remains within reference limits and that patient protection is upheld (Omar et al., 2019). In skull radiography, the posteroanterior (PA) projection can reduce the absorbed dose to the eyes by up to 95% compared to the anteroposterior (AP) projection (IAEA, 2002). Some skull projections require caudal angulation of the X-ray tube to minimise thyroid dose, and beam collimation helps reduce unnecessary radiation to the thyroid gland. Research has shown that the use of shielding significantly reduces thyroid doses (Shortt et al., 2008).

Moreover, there are various techniques to reduce radiation dose in skull X-ray examinations, including decreasing the collimator field size, using more sensitive detectors, and implementing the air gap technique (Tsuji et al., 2006). While the use of anti-scatter grids can enhance image quality, it typically increases the dose by 50%, as higher X-ray intensity is required to maintain the signal-to-noise ratio (SNR) (IAEA, 2002). Increasing the object-to-image distance (OID) through the air-gap technique reduces scattered effects and contributes to improved image quality, although it may magnify the image.

In the field of radiological practice, the issue of radiation dose during skull radiography has become a subject of debate due to the use of low exposure factors. While the doses may appear low, there are concerns regarding the direct primary beam exposure to the eyes and scattered radiation affecting areas outside the collimated region, such as the thyroid gland. Protecting these sensitive organs, the thyroid and eyes, is of paramount importance during skull imaging (Omar, M et al., 2019). Chang et al. (2017) mentioned that conventional radiography, particularly in skull can result in the thyroid gland receiving significant doses of radiation. Moreover, a study by Omar, N. A. et al. (2019) highlighted the potential for x-ray exposure to impact the eyes' lenses, leading to eye problems.

This study aims to measure the radiation dose received by the skull, eyes, and thyroid during skull X-ray procedures by employing optically stimulated luminescence dosimeters (OSLD). The study employs both anti-scatter grid and non-grid techniques (air gap technique). Importantly, this research excludes shielding for the thyroid. The anti-scatter grid plays a crucial role in improving image quality by selectively rejecting scattered radiation while transmitting primary radiation. In summary, the primary goals are to gain insights into optimising radiation dose and image quality in skull radiography, with a focus on enhancing patient safety and minimising radiation exposure while maintaining diagnostic image quality.

MATERIALS AND METHODS

In this experimental study, Siemens MULTIX TOP X-ray imaging system was employed. The Kyoto Kagaku Anthropomorphic PBU-50 head phantom was exposed. To accurately simulate the positioning of a patient with a traumatic head injury, the PBU-50 head phantom was placed in a supine position on the bucky table, which was oriented for an anteroposterior (AP) projection as shown in Figure 1. This supine presentation closely resembles the posture adopted by patients in trauma conditions, especially when a skull examination is required. A 24 x 30 cm image receptor (IR) was carefully positioned lengthwise on top of the bucky table. This precise placement is vital in capturing the entire area of interest in the skull examination. The choice of exposure factors, specifically kilovoltage peak (kVp) and milliampere-seconds (mAs) settings, was influenced by prior research conducted by Khoshdel-Navi et al., (2016).

Figure 1. Shows the PBU-50 head phantom on the bucky table with grid (no air gap).

According to Khoshdel-Navi et al., (2016) the acceptable range of exposure factors for the AP skull projection is 60 to 78 for kVp and 8 to 50 for mAs. In this study, two kVp settings, namely 68 kVp and 75 kVp, were selected. Additionally, mAs adjustments were made, with 9 mAs and 12.5 mAs applied for both methods. The source-to-image receptor distance (SID) of 100 cm and a small focal spot size was selected. A summary of these parameters can be found in Table 1.

Table 1. Parameters used in this experimental study

PARAMETERS	DETAILS
Kilovoltage (kVp)	68, 75
Milliampere-second (mAs)	9, 12.5
Imaging plate size (cm)	AP projection: 24 x 30, lengthwise
Central ray	Perpendicular to the center of IR, AP projection: at the level of glabella
Source-to-image distance (cm)	100
Object-to-image distance (cm)	0, 4
Focal spot	Small focal spot
Grid (grid ratio)	Stationary grid (8:1)
AEC	Off

For non-grid technique with a 4cm air gap (OID). The head phantom was positioned directly onto the imaging plate, with a 4cm air gap achieved using a skull foam positioning pad. Sponges were placed on both sides of the head phantom to immobilise it as shown in Figure 2.

Figure 2. Shows the PBU-50 head phantom on the bucky table without grid with air gap (4cm OID)

To measure the ESD naonDot OSLDs were placed at specific locations; glabella, eyes, and thyroid on the skull as shown in Figure 3A and B. Before the exposure to the OSLD process was conducted, an initial reading of the OSLD was taken and recorded. This initial reading was documented in a lab logbook. To determine the ESD, the result of the post-irradiated dosimeter was subtracted from the initial reading. This calculation provided the radiation dose at the entrance surface of the tissue. Each exposure and dose reading were repeated three times for each kilovoltage peak (kVp) used, and an average dose reading was calculated. This repetition ensured accuracy in the measurements. The experiment involved variations in the use of grids and object-to-image distance (OID). Figure 3 (A) depicts the setup with a grid - no air gap, while Figure 3 (B) shows the setup without a grid and with a 4cm OID – air gap.

Figure 3. Positions of nanoDot OSLDs on PBU-50 head phantom for the measurement of ESD with a grid (A) and without a grid (B).

For image quality assessment a total of 8 images were obtained using the technical parameters summarised in Table 1 and subsequently evaluated by four experienced radiographers. To ensure the competency of the radiographers conducting the evaluation, a minimum requirement of at least 2 years of experience in the radiography field was set. To maintain objectivity and prevent bias during the evaluation process, the images were intentionally labelled with 8 alphabet codes, concealing any information regarding the technique and exposure factors used to capture the images. This practice aimed to ensure that the evaluation was solely based on the image quality and not influenced by any extraneous factors. Each of the four radiographers received a set of evaluation forms (as detailed in Table 2) for their individual assessment of the images. The evaluation process employed the Image Criteria Scoring (ICS) method, focusing on image quality criteria relevant to AP skull images, including clarity, contrast, and anatomical details.

Table 2. Shows the Image Criteria Scoring (ICS) method and image quality criteria.

No	Criteria	Scale	Image Quality
1	Visually sharp reproduction of apex of petrous temporal bone	1	Very poor
2	Visually sharp reproduction of outer and inner lamina of cranial vault	2	Poor
3	Visually sharp reproduction of inner auditory canal	3	Fair
4	Overall contrast	4	Good
5	Overall density	5	Excellent
6	Overall image resolution		

IBM's Statistical Package for the Social Sciences (SPSS) version 26 was used to compile and analyse the study's data. The resulting ESD and the image quality of the AP skull projections using the grid approach and the non-grid technique with an OID increase were compared using the Kruskal-Wallis test for statistical significance.

RESULTS

Entrance Surface Dose (ESD) to Skull in AP Skull Examination

Entrance surface dose (ESD) for anterior-posterior (AP) skull radiography was investigated under different exposure factors, and comparing the use of a grid technique without air gap (0 cm OID) and without a grid technique with 4 cm air gap (OID). The study aimed to assess the impact of grid usage and OID variation on ESD and to understand how variations in kVp and mAs affect ESD. The key findings are as follows:

Figure 4 presents the mean ESD values for AP skull radiography with a grid and no grid (4 cm air gap). The ESD for the skull was slightly higher when no grid was utilized, indicating that the grid technique effectively reduced ESD. This observation aligns with the intended purpose of grids in radiography, which is to minimize scattered radiation. The ESD decreased when kVp was increased with low mAs, demonstrating that higher-energy X-rays (kVp) can produce diagnostic images with reduced radiation exposure.

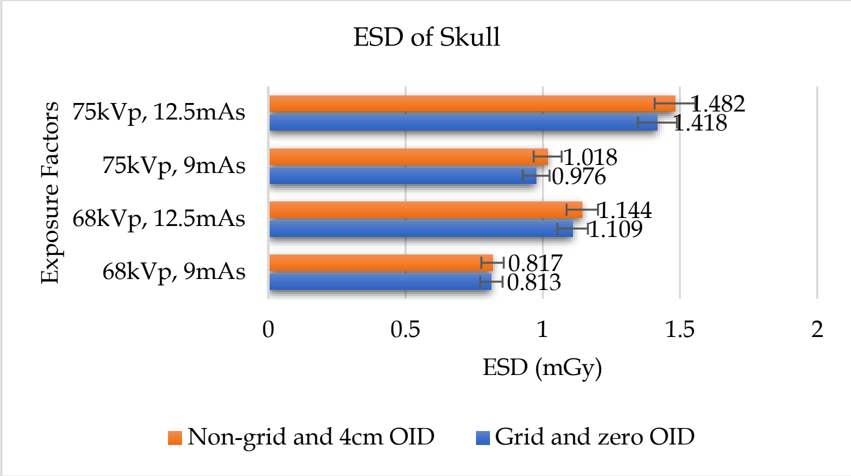

Figure 4. Mean ESD of AP skull with a grid (no air gap) and without a grid at 4 cm air gap (OID)

Conversely, when the same kVp was used with higher mAs, ESD increased, highlighting the direct relationship between mAs (exposure) and ESD. The radiographic settings of 75 kVp and 12.5 mAs caused the highest ESD to the skull. This was true for both grid and no grid techniques, with values of 1.418 mGy and 1.482 mGy, respectively. The Kruskal-Wallis test was conducted. The statistical analysis revealed that there was no statistically significant difference in the average ESD between the skull imaging conducted using the grid approach without object-image distance (OID) and the non-grid technique with a 4 cm OID. The p-value obtained from the analysis was 0.564, which is more than the predetermined significance level of 0.05.

Radiation Dose to Eyes in an AP Skull Examination

According to the findings of the study, the AP skull examination without a grid resulted in a higher eye dosage of 1.558 mGy at 75 kVp and 12.5 mAs as shown in Figure 5, whereas the grid technique with lower exposure factors (68 kVp and 9 mAs) resulted in the lowest eye dose of 0.82 mGy. The grid approach also resulted in the lowest overall eye dose.

Radiation Dose to Thyroids in an AP Skull Examination

Figure 6 shows the highest measured dosage to the thyroid gland was 0.039 mGy (75 kVp, 12 mAs, no grid and 4 cm air gap), while the lowest dose measured was 0.015 mGy (68 kVp, 9 mAs, no grid, and 4 cm air gap). The thyroid gland, situated at a greater distance from the centre beam, was exposed to comparatively lower dosages for each specific technical configuration. The investigation employed a standardised collimation size and deliberately omitted the thyroid gland from the region covered by the collimation beam in order to reduce the extent of thyroid exposure.

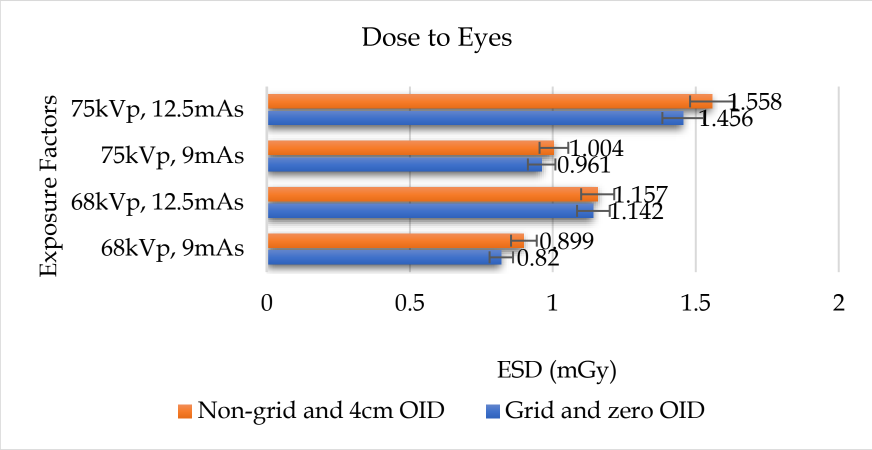

Figure 5. Mean doe to eyes with a grid (no air gap) and without a grid at 4 cm air gap (OID).

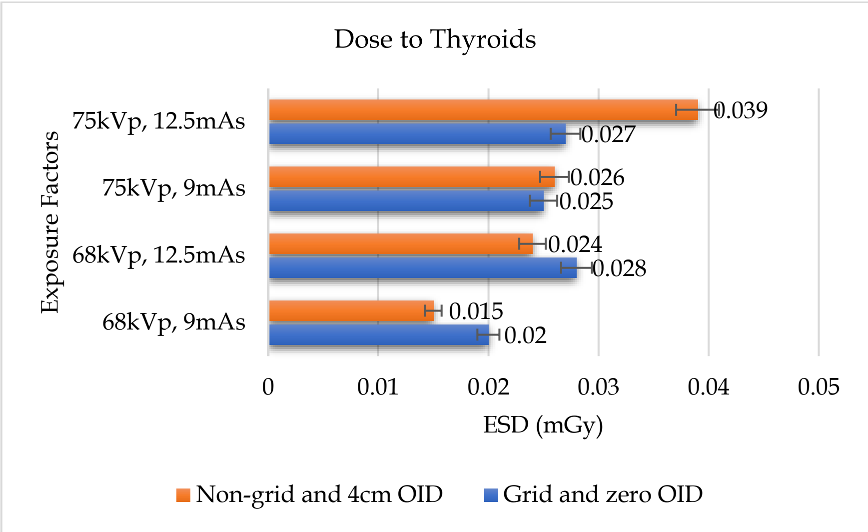

Figure 6. Mean doe to thyroids with a grid (no air gap) and without a grid at 4 cm air gap (OID).

Radiographic Images of the Anteroposterior (AP) Skull Projection

The images were obtained by varying the exposure settings with and without a grid. The acquisition of images for the AP skull projection aims to achieve optimal image quality while capturing diagnostically relevant features. The radiographs labelled as A, B, C, and D, as seen in Figure 7, pertain to the anteroposterior (AP) skull imaging approach utilising a grid and a no air gap (0 cm OID). The radiographs depicted in Figure 8 (A, B, C and D) correspond to the AP skull imaging, specifically utilising the non-grid technique with an air gap of 4 cm (OID). It is important to acknowledge that the exposure factors employed in this investigation were derived from clinical settings.

The primary aim of this part of the study was to determine the effects of AP skull radiography, specifically focusing on identifying the technique that offers the lowest exposure factor and optimal image quality. To accomplish the objective of this study, a group of four radiographers performed an evaluation of the image quality. The results were synthesised and subsequently shown in Figure 9.

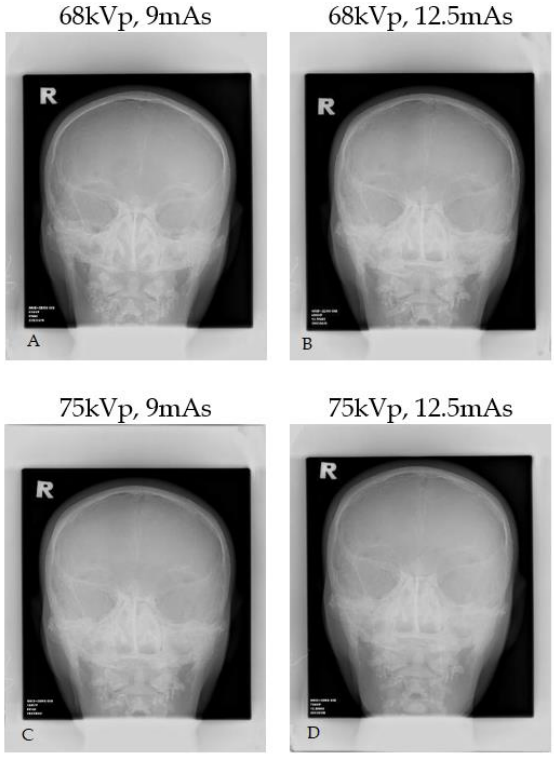

Figure 7. Radiographs of AP Skull with Grid Technique

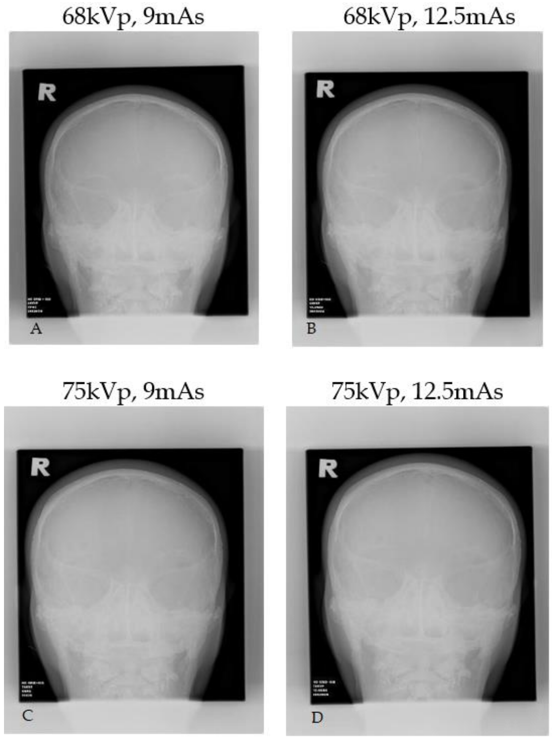

Figure 8. Radiographs of AP Skull without Grid Technique and 4cm OID

The results of the Kruskal-Wallis test revealed a statistically significant disparity in image quality when comparing the utilisation of grid and non-grid approaches in relation to the 4 cm air gap (OID) of the score derived from the ICS assessment in AP skull radiography ($p = 0.02$, $p<0.05$).

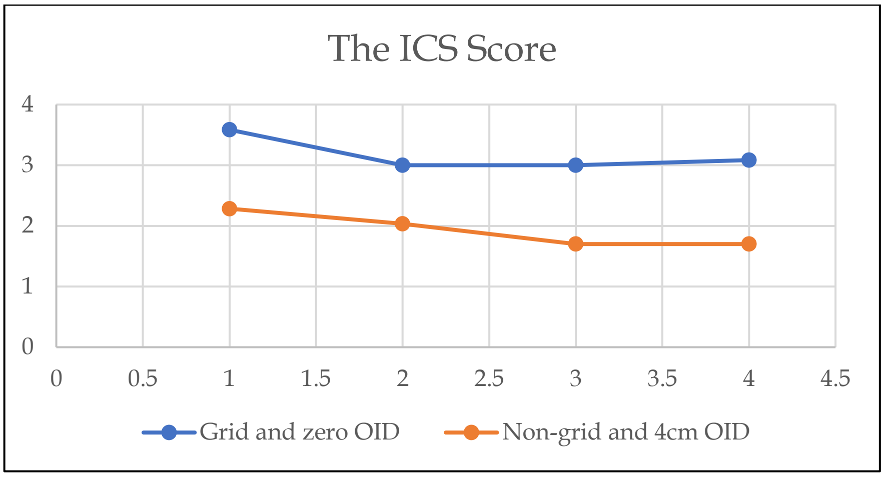

Figure 9. Average of Image Criteria Scoring (ICS) for AP skull radiography by using grid and non-grid with OID technique with different exposure factors (kVp and mAs)

DISCUSSION

In diagnostic imaging, X-ray photons interact with matter in two main ways: photoelectric absorption and the Compton Effect. These effects are mainly determined by the energy of the X-ray photons that hit the material (Carlton & Adler, 2013). Tube potential (kVp) and milliampere-seconds (mAs) are essential parameters in X-ray production. Tube potential (kVp) determines the energy of the X-ray photons, affecting image contrast and patient dose (Martin, 2007). Milliampere-seconds (mAs), on the other hand, determines the amount of radiation produced over time, influencing radiographic image density.

The study results revealed that using high kVp with low mAs settings resulted in lower entrance skin dose (ESD) compared to lower kVp with high mAs settings. High kVp increases the energy of the photons, allowing them to penetrate deeper and exit the patient's body without significant absorption by tissues, resulting in lower ESD. Conversely, lower kVp with high mAs leads to higher ESD due to increased photoelectric absorption in body tissues.

ESD of Skull with Grid at 0cm OID and without Grid at 4cm OID

The highest recorded ESD for skull X-ray was 1.482 mGy, using exposure factors of 75 kVp and 12.5 mAs without a grid technique. However, this value is still below the Diagnostic Reference Level (DRL) of 4.8 mGy set by the Ministry of Health Malaysia (2013) for anterior-posterior (AP) skull radiography. The use of an air-gap technique without a grid reduced patient surface exposure compared to using a grid. The study's results showed only a slight difference in ESD between the grid and non-grid techniques at a 4 cm object-to-image distance (OID), with slightly higher values for the non-grid technique.

The study used medium-level exposure factors, specifically kVp in the range of 68–75 kVp, and did not employ high kVp techniques. Generally, 75 kVp settings resulted in a slightly higher ESD. Nonetheless, the doses remained within acceptable limits based on various studies, Table 3. Differences in techniques, patient characteristics, exposure settings, dosimeter types, and dosimeter placement across studies might account for slight variations in ESD measurements.

Table 3. Comparison of measured ESD to skull in AP skull examination with the other studies.

Projection	**ESD (mGy)**			
	This study	Mohamadain et al., (2015)	Suliman et al., (2006)	Compagnonet al., (2008)
AP Skull	0.81-1.48	0.66-1.25	1.41-2.26	1.32-1.64

These findings suggest that this specific combination of 75 kVp and 12.5 mAs resulted in the highest radiation exposure to the skull. When using 68 kVp with 9 mAs, the ESD to the skull for both grid and no grid techniques was the lowest at 0.813 mGy and 0.817 mGy, respectively. This combination of settings minimized radiation exposure to the skull.

These findings underscore the importance of optimizing radiographic techniques to minimize radiation doses while maintaining image quality. Using grids effectively reduces ESD, which is critical for patient safety. Furthermore, selecting appropriate combinations of kVp and mAs is essential to achieving diagnostic images while keeping radiation exposure as low as reasonably achievable (ALARA). This research work offers significant contributions by shedding light on the variability of dose in anteroposterior (AP) skull radiography, hence providing useful guidance for optimising radiation dosage in clinical environments.

Dose to the Eyes and Thyroid with and without the Grid Technique

Eyes

Radiation exposure is a critical concern in medical imaging, particularly for procedures involving the head. This section discusses the findings of our study on radiation dose in anterior-posterior (AP) skull X-rays and compares them with a related study by Saeed and Almalki conducted in 2022. The objective of the study was to assess how variations in exposure factors, such as kilovoltage peak (kVp) and milliampere-seconds (mAs), impact the radiation dose to the eye lens.

The study revealed significant variations in eye lens dose depending on the selected kVp and mAs values. When using higher values of kVp (75) and mAs (12.5) for skull X-rays, the eye lens dose increased. Specifically, the highest eye dose measured in this study was 1.558 mGy during AP skull examinations performed without the use of a grid. Conversely, the lowest dose recorded was 0.82 mGy, achieved with a grid technique and lower exposure factors (68 kVp and 9 mAs). Despite these variations, all measured doses remained below the established threshold dose range of 0.5 to 2.0 Gray (Gy) associated with the development of eye lens opacities.

Compared to Saeed and Almalki (2022), who used DoseCal and CALDose_X software to measure radiation doses to the eyes during AP skull examinations. Their findings reported doses of 2.2 mGy and 2.5 mGy, respectively. It becomes clear from comparing these outcomes to the doses measured in our study that the doses we obtained were lower than those Saeed and Almalki reported. This suggests that the choice of equipment, technique, and exposure factors can significantly impact radiation doses to the eye lens during AP skull X-rays.

Radiation dose management is of paramount importance in medical imaging to minimize potential health risks to patients. The study discussed here demonstrates the significance of exposure factors such as kVp and mAs in influencing eye lens doses during AP skull X-rays. Despite variations, all measured doses remained below the threshold dose associated with eye lens opacities. Furthermore, a comparative analysis with a previous study indicates the potential for optimization of radiation doses to the eyes, emphasizing the importance of choosing appropriate equipment and techniques for such procedures.

Thyroids

Radiological imaging plays a critical role in modern medicine for diagnostic and therapeutic purposes. However, it is essential to consider the potential radiation exposure to sensitive organs. Among the various organs vulnerable to radiation, the thyroid gland is of particular interest due to its location in the neck and its sensitivity to ionizing radiation. Our study investigated thyroid radiation doses in AP skull examination and how various factors, including technological advancements, have contributed to minimizing thyroid exposure. Additionally, historical data is presented to provide context for the study's results.

An important part of the study looked at how radiation dose patterns, especially kVp (kilovolt peak) and mAs (milliampere-seconds), affect thyroid doses. The results revealed that higher kVp and mAs settings correlated with increased thyroid doses, with the maximum recorded dose being 0.039 mGy and the lowest being 0.015 mGy. Interestingly, the thyroid, situated farther from the central ray, received relatively lower doses for each technical setting as compared to eyes. This variation underscores the importance of optimizing imaging parameters to minimize thyroid exposure.

To minimize thyroid exposure, the study employed various strategies. It utilized a fixed collimation size and excluded the thyroid from the collimation beam area, effectively shielding it from unnecessary radiation. Additionally, factors such as the number of projections and mAs were identified as influencing thyroid doses, emphasizing the importance of precise and tailored settings during imaging procedures.

Melo et al. (2016) presented historical patient data from 1930 to 2009 in order to contextualize the significance of the study's findings. According to this historical data, the average thyroid dose for the years 2000–2009 was 0.42 mGy. This historical perspective highlights a remarkable reduction in thyroid radiation exposure over the years. The study acknowledges that several technological advancements have played a pivotal role in achieving a noteworthy decrease in thyroid radiation exposure over time. These advancements include the implementation of collimators, filters, films, and intensifying screens, which collectively contribute to enhancing radiation safety in medical imaging.

Collimators are instrumental in shaping and limiting the X-ray beam, ensuring that only the necessary area is exposed to radiation. Filters are used to selectively absorb low-energy X-rays, further reducing unnecessary radiation exposure. Films and intensifying screens work together to improve image quality while reducing the amount of radiation required to obtain diagnostic images.

In summary, the study on thyroid radiation doses underscores the importance of optimizing imaging parameters and employing technological advancements to minimize radiation exposure to the thyroid gland. The historical context presented by Melo et al. (2016) reveals a significant reduction in thyroid doses over the years, showcasing the effectiveness of these measures in enhancing patient safety during medical imaging procedures. By adhering to best practices and leveraging technological innovations, healthcare providers can continue to ensure that thyroid radiation exposure remains at safe and minimal levels, thereby safeguarding the health and well-being of patients.

Image Quality of AP Skull Radiographs with and without Grid Technique

The image quality of AP skull radiographs with and without grid technique, reveals important insights into the impact of various radiographic techniques on image quality in skull radiography. The analysis of the findings provide a deeper understanding of the implications.

The study clearly demonstrates that the use of a grid technique significantly improves the image quality in skull radiography. The images taken with the grid technique consistently received higher scores from the evaluators compared to those without the grid or using the air-gap technique. This finding aligns with previous research indicating that grids are effective in reducing scatter radiation, which can degrade image quality (Bushberg et al., 2013).

Additionally, the research indicates that the use of the air-gap technique as a potential alternative to the grid may necessitate modifications in the characteristics of such approach. The the 4 cm OID employed in this investigation may have played a role in diminishing the quality of the images obtained using the air-gap approach. This is because scattered photons were able to reach the image receptor, so impacting the overall contrast and resolution. In order to raise the efficacy of the air-gap approach, it may be imperative to modify technical parameters or increase the OID to optimise the elimination of scattered radiation.

In addition, a greater number of scattered photons may reach the detector due to Compton scattering, which becomes more prevalent at higher kVp levels. Image noise is reduced and quality is enhanced because of grids' ability to absorb scattered radiation before it reaches the detector. Consequently, the findings of this study align with the aforementioned phenomena (Bushberg et al., 2013).

Moreover, the results of this study suggest that tube voltage (kVp) plays a crucial role in controlling contrast in skull radiography. Higher kVp values result in greater penetration of X-rays through the patient's tissues, which can affect image contrast. The study's findings support the principle that subject contrast, related to the differences in X-ray absorption by various tissues, is influenced by kVp selection (Schueler, 1998). For instance, the image at 75 kVp with 12.5 mAs showed slightly lower contrast compared to the image at 68 kVp with 9 mAs. This reinforces the importance of optimizing kVp settings to achieve the desired image contrast.

Additionally, the study highlights that mAs selection primarily affects image density but also has a secondary influence on contrast. Over exposure and under exposure can lead to reductions in image contrast. In this study, both 9 mAs and 12.5 mAs were considered for skull radiography, emphasizing the importance of appropriate mAs selection to achieve optimal image quality.

Furthermore, the findings of the research work show that using medium kVp selection along with the grid technique improves the visibility of important anatomical structures in skull x-rays, like the petrous temporal bone and the inner lamina of the cranial vault. This finding has clinical significance, as it suggests that specific technique parameters can improve the diagnostic value of skull radiographs.

In summary, this study provides valuable insights into the factors affecting image quality in skull radiography. It proves that the grid technique works to cut down on scatter radiation, stresses how important it is to choose the right tube voltage and mAs for contrast control, and stresses how important it is to use the right OID in the air-gap technique. These findings have implications for radiographic practice, emphasizing the importance of optimizing technique parameters to achieve high-quality skull radiographs and improve diagnostic accuracy.

CONCLUSION

This study has provided valuable insights into the use of grid technique and non-grid technique with a 4 cm air gap technique in anterior-posterior (AP) skull examinations. While no significant differences were observed in entrance surface dose (ESD) between the grid and non-grid techniques, the application of the grid led to significantly enhanced image quality. Further, the study also showed that using the lowest exposure factors produced the highest image quality. Notably, the ESD was higher when the skull phantom was close to the X-ray source and a non-grid technique was used with a 4 cm OID. Moreover, the dose for critical organs like the eyes and thyroid gland was also remarkably elevated when using the non-grid technique. This suggests that, from a radiation safety perspective, employing the grid technique is not only beneficial for image quality but also for minimising unnecessary radiation exposure to the thyroid and eyes. Additionally, the use of the grid technique also ensures improved visualisation of critical regions such as the petrous temporal bone and inner auditory canal, as well as density and contrast throughout the image. This highlights the potential for optimising radiation doses for patients while adhering to the "As Low As Reasonably Achievable" (ALARA) principle. In summary, the findings from this study emphasise the significance of employing the grid technique for AP skull radiography to achieve superior image quality and optimise radiation exposure for patients. This not only enhances diagnostic accuracy but also ensures patient safety by minimising unnecessary radiation exposure to sensitive organs. Furthermore, these results underscore the importance of adhering to the ALARA principle and adopting the right technique for the benefit of both patients and healthcare practitioners.

REFERENCES

Bushberg, J. T. et al. (2013). The Essential Physics of Medical Imaging. Lippincott Williams & Wilkins

Carlton, R. R., & Adler, A. M. K. (2013). Principles of radiographic imaging: an art and a science (5th ed.). Delmar/Cengage Learning.

Chang, W., et al. (2017). Thyroid Dose from Common Head and Neck CT Procedures in Children: Impact of Radiation Dose Reduction. AJR. American Journal of Roentgenology, 209(2), 416-421.

Compagnone, G., Pagan, L., Baleni, M. C., Calzolaio, F. L., Barozzi, L., & Bergamini, C. (2008). Patient dose in digital projection radiography. Radiation Protection Dosimetry, *129(1-3), 135–137.* doi:10.1093/rpd/ncn013

Donya, M., Radford, C., ElGuindy, A., Firmin, D., & Yacoub, M. (2014). Radiological dose optimization during cardiac catheterization procedures. Journal of Medical Imaging and Radiation Sciences, 45(2), 171-178.

Fetterly, K. A., Schueler, B. A., Grams, M. P., Stone, M. R., & Lennon, A. M. (2017). Impact of Lead Apron Use on Radiation Dose to the Radiologist in the Neurointerventional Suite. American Journal of Roentgenology, 208(2), 408-412.

Gogos, C., Papadimitriou, D., Bousbouras, P., & Papadopoulou, A. (2013). Quality assurance in diagnostic radiology: the role of the medical physicist. The British Journal of Radiology, 86(1026), 20130039.

IAEA. (2002). Radiation Protection in Diagnostic Radiology. International Atomic Energy Agency.

IBM Corp. (2019). IBM SPSS Statistics for Windows (Version 26.0). IBM Corp.

Karami, V., Zabihzadeh, M., Shams, N., Keshtkar, M., & Aghamiri, M. R. (2017). A Comprehensive Review of Radiation-Induced Tumors. Journal of Biomedical Physics & Engineering, 7(3), 243-252.

Khoshdel-Navi D. et al. (2016). Local-Reference Patient Dose Evaluation in Conventional Radiography Examinations in Mazandaran, Iran. J Biomed Phys Eng 2016; 6(2): 61-70.

Martin, C. J. (2007). Optimisation in general radiography. In Biomedical Imaging and Intervention Journal. https://doi.org/10.2349/biij.3.2.e18

Mazonakis, M., Tzedakis, A., Damilakis, J., & Gourtsoyiannis, N. (2004). A quality assurance program for radiographic and fluoroscopic equipment. Radiation Protection Dosimetry, 110(1-4), 509-515.

Melo, D.R. et al. (2016). Organ Doses From Diagnostic Medical Radiography—Trends Over Eight Decades (1930 to 2010). Health Physics. 2016; 111(3): 235–255. DOI: 10.1097/HP.0000000000000524

Ministry of Health Malaysia. Malaysian Diagnostic Reference Levels (DRLs) in Medical Imaging (Radiology), 2013.

Mohamadain, K.E.M., Habbani, F.I. and Ibrahim, S.M. (2015) Adult Patient Doses for Chest, Skull and Lumbar Spine Examinations. Open Journal of Radiology, 5, 44-49. http://dx.doi.org/10.4236/ojrad.2015.51008

Omar, M., et al. (2019). Impact of X-ray Radiation Exposure on Thyroid and Eyes. International Journal of Recent Scientific Research, 10(2), 30797-30802.

Omar, N. A., Samat, S. B., Ismail, B., & Hashim, S. (2019). Optimization of radiation dose in computed tomography for pediatric head examination using the image quality assessment. Radiography, 25(3), 216-221.

Saeed, M. K and Almalki, Y. (2022). Assessment of the radiation dose associated with X-ray examinations using the DoseCal and CALDose_X software packages. International Journal of Radiation Research. *20(1): 191-197* DOI: 10.52547/ijrr.20.1.29

Schueler, B. A. (1998). Clinical applications of basic x-ray physics principles. RadioGraphics. https://doi.org/10.1148/radiographics.18.3.9599394

Shortt, C. P., Ryan, D., Purtill, D., & O'Kelly, P. (2008). Radiation dose to the eye lens from cerebral and cervical angiography: determination of left and right eye dose and an estimate of detriment. American Journal of Neuroradiology, 29(5), 816-822.

Suliman, I. I., Abbas, N., & Habbani, F. I. (2006). Entrance surface doses to patients undergoing selected diagnostic X-ray examinations in Sudan. Radiation Protection Dosimetry, 123(2), 209–214. doi:10.1093/rpd/ncl137

Tsuji, S. Y., Cagnon, C. H., & Rong, J. (2006). Comparison of patient doses in full-field digital mammography and screen-film mammography in a general daily practice using the IAEA patient dosimetry method. Radiation Protection Dosimetry, 118(1), 61-67.